

• Technology and Methods •

Application of dynamic contrast enhancement MRI and post-processing technique for diagnosis of breast cancer

Kang-Qiang Peng,^{1,2} Zi-Lin Huang,^{1,2} Chuan-Miao Xie,^{1,2} Lin Chen,^{1,2} Yi Ouyang,^{1,3}

Qing-Sheng Zheng,^{1,2} Yan Zhang,^{1,2} Hao-Qiang He^{1,2} and Pei-Hong Wu^{1,2}

1. State Key Laboratory of
Oncology in South China,
Guangzhou, Guangdong, 510060,
P. R. China

2. Department of Imaging and
Interventional Radiology,
Cancer Center,
Sun Yat-sen University,
Guangzhou, Guangdong, 510060,
P. R. China

3. Department of Radiation
Oncology, Cancer Center,
Sun Yat-sen University,
Guangzhou, Guangdong, 510060,
P. R. China

Correspondence to: Chuan-Miao Xie

Tel.: 86.20.87343217

Email: xchuanm@mail.sysu.edu
.cn

This paper was translated into English
from its original publication in Chinese.

Translated by: Beijing Xinglin Meditrans
Center (<http://www.51medtrans.com>)
and Jun Ma

The original Chinese version of this paper
is published in: Ai Zheng (Chinese Journal
of Cancer) 28(5); [http://www.cjcsysu.cn/cn/
article.asp?id=15354](http://www.cjcsysu.cn/cn/article.asp?id=15354)

Submitted: 2008-04-02

Revised: 2008-10-07

[Abstract] **Background and Objective:** Magnetic resonance imaging (MRI), an advanced non-invasive technique, is regarded as one of the potential modalities in the diagnosis of breast cancer. This study was to investigate the application of dynamic contrast enhancement MRI and 3D reconstruction images in diagnosing breast tumors. **Methods:** From May 2006 to September 2007, 30 patients with breast diseases were scanned with MRI in Sun Yat-sen University Cancer Center. MR plain scans, dynamic contrast enhancement scans were performed, and 3D reconstruction images were obtained. The normal breast tissue was used as control, and the maximum slope ratio was calculated. **Results:** Forty-nine lesions were found in 30 patients, with an accuracy rate of 93.3%. **Conclusion:** MRI scan is an effective and specific modality for the diagnosis of breast diseases with high sensitivity and accuracy. Dynamic contrast enhancement MRI, image subtraction, time-signal intensity curve, 3D reconstruction images and the maximum slope ratio are helpful to make the correct diagnosis of breast lesions.

Key words: Breast neoplasm, MRI, dynamic contrast-enhanced, post-processing technique, diagnosis

Breast cancer is the most common malignancy among women, the incidence of which increases over the years.¹ Magnetic resonance imaging (MRI) is a non-invasive imaging technique. It has been rapidly developed over the past decade and is regarded as the most potential examination modality for diagnosis of breast cancer. There is no agreed-on imaging mode for breast MRI since the techniques are varied and complicated. However, most radiologists believe consecutively 3 to 10 min of T₁-weighted MRI following bolus intravenous injection of gadopentetate dimeglumine (Gd-DTPA), besides plain breast MRI scan and contrast enhanced MRI, can evaluate morphology and hemodynamics of the breast. The post-processing techniques including image subtraction, dynamic curves mapping and three-dimensional (3D) reconstruction help to find and identify breast lesions and qualitative diagnosis of them as well.^{2,6}

The current study aimed to investigate application of plain MRI

and dynamic contrast enhanced MRI and post-processing techniques for diagnosis of breast tumors.

Materials and Methods

Clinical samples. We included 30 patients with newly diagnosed breast disease who underwent breast MRI at Sun Yat-sen University Cancer Center between May 2006 and September 2007. All were females aged 26-67 years with a median age of 40 years old.

Imaging protocol. Breast MRI was performed on a 1.5-T system (GE, Signa CV/I, excite II) with a dedicated breast surface coil (four-coil phased array). After measurement of weight and removal of metal objects, an intravenous catheter was placed in dorsal superficial veins of hand before the MRI began. The patients were required to lie in a prone position to rest the breasts in two cushioned holes of the breast coil, with feet first into the machine.

Initially, fast spin echo (FSE) T1-weighted images (T1WI) in the transverse and sagittal planes [repetition time (TR): 650 milliseconds; echo time (TE): Min Full; echo train length (ETL): 2; bandwidth (BW): 20.83] and FSE T2-weighted images (T2WI) in the transverse and sagittal planes (TR: 4650 milliseconds; TE: 85 milliseconds; ETL: 16 and BW: 20.83) were obtained before injecting the contrast material. The section thickness was 6 mm and the section spacing was 1mm. The field of view (FOV) was adjusted according to the size of the breast, ranging from 180 mm × 180 mm to 280 mm × 280mm. The acquisition matrix size was 320 × 224. The Freq double-inversion-recovery (DIR) was set to A/P and the number of repeated excitations (NEX) was 2. Except the transverse T1WI, all the other sequences were fat-suppressed.

After plain MRI scan, the dynamic contrast enhanced MRI was performed as follows: 1) when the pre-scanned images were desirable, the dynamic enhanced MRI was performed. The high pressure injector and dynamic scanner buttons were initiated simultaneously; 2) The

Gd-DTPA was administered through the intravenous catheter with the high pressure injector (Medrad Injector System, Medrad, PA, US) (dose: 0.1mmol/kg; and speed: 3ml/s). A 10-ml saline flush followed the bolus injection at a speed 3ml/s; 3) The areas of lesions were scanned in the transverse and sagittal planes for 3D liver acquisition with volume acceleration (LAVA). The parameters were listed as follows: pulse sequence: 3D fast time-of-flight (TOF) spoiled gradient-echo (SPGR); fractional anisotropy (FA): 12; BW: 83.33; acquisition matrix: 288 × 288; FOV: 38; Phase FOV: 0.90; Freq DIR: A/P; Multi-phase: 10, Zip × 2, time resolution: about 20 s; section thickness: 2.8 mm; and Locs per spacing: 50 mm; 4) the dynamic contrast enhanced MRI lasted around 5 min.

After dynamic contrast enhanced MRI scan, transverse and sagittal fat-suppressed T1WI sequences were performed.

MRI Post-processing and image interpretation. Two professional MRI radiologists post-processed the dynamic contrast enhanced MRI in a blind manner, observed and measured relevant data using the Function Tool Image analysis package (General Electric, WI, US).

- 1) The dynamic MR images were transferred to the workstation. Different areas of the images were colored differently to reflect the intensities, as plotted in the pcolor;
- 2) The subtracted MR images were from enhanced MR images subtracted by the plain MR images;
- 3) With the breast lesions as the areas of interest, the areas of necrosis and calcification were deleted. The signals of the breast lesions were consecutively collected. The intensity-time curves were generated using the post-processing procedures;
- 4) Appropriate images were selected for 3D reconstruction;
- 5) The maximum slope ratio was calculated as per $\text{SlopeR} = (\text{SI}_{\text{postf}} - \text{SI}_{\text{pref}}) / (\text{SI}_{\text{postn}} - \text{SI}_{\text{pren}})$ (where SI_{post} was the highest signal intensity in the scanning period when the signal increase span was the highest; SI_{pre} was the lowest signal intensity in the same scanning period; and

subscript f signified focus and n signified normal tissue). For SlopeR, the distant normal tissues from the lesions were taken as the contrast. Regarding the regressive breast, the distant fat tissues from the lesions were selected; while for the non-regressive breast, the distant breast tissues from the lesions were selected.

Post-processing techniques for breast MRI. Pcolor. The pcolor was an image presenting areas of different signal intensities of various sites or degrees with different colors via the workstation.

Subtracted image. The subtracted image was from the contrast enhanced image subtracted by the plain image in the same plane, showing areas of signal intensity changes between these two images.

Intensity-time curve. The intensity-time curve was plotted with the signal intensity by the time.

3D reconstruction image. The 3D reconstruction image was the 3D outcome of overlying images in the same sequence using a 3D reconstruction tool.

Calculation of maximum slope ratio. The maximum slope ratio was calculated as per $\text{SlopeR} = (\text{SI}_{\text{postf}} - \text{SI}_{\text{pref}}) / (\text{SI}_{\text{postn}} - \text{SI}_{\text{pren}})$. The distant normal tissues from the lesions were taken as the contrast so that variance of individuals was avoided and then the maximum slope ratio reflected characteristics of the lesions in a more accurate manner and with more comparability.

Results

In the current study, 49 lesions were observed in 30 patients. 15 patients had 1 lesion individually, 6 had 2 lesions individually, 6 had 3 lesions each, 1 had 4 lesions and 2 had none. The diagnosis accuracy rate was 93.3% (Table 1).

Pathological diagnosis. 12 patients were diagnosed as having breast cancer with a total of 26 lesions (53.1%), of whom one was diagnosed as having inflammatory breast cancer and the other 11 were diagnosed as infiltrating ductal carcinoma. Of these 11 patients, 1 had lymph node metastasis, 2 showed axillary lymph node

metastasis with invasion to chest wall or musculi pectoralis major, 2 was accompanied with fibroadenoma, 1 with fibroadenosis, 1 with cyst, and 1 with invasion to skin and papilla.

15 patients were diagnosed as having benign diseases with 22 lesions (44.9%). Of them, 3 had fibroadenoma, 1 fibroadenoma plus cyst, 1 fibroma, 2 intraductal papilloma, 1 fibroadenoma plus intraductal papilloma, 1 cyst, 1 lobule hyperplasia adenosis, 1 fibrocystic hyperplasia, 1 sclerosing adenosis, and 3 inflammation.

1 patient had prosthesis with 1 lesion (2.0%) and 2 patients had no lesions.

MRI diagnosis. Characteristics of plain and contrast enhanced MRI of the breast diseases. Plain breast MRI included 6 sequences: transverse T1WI and T2WI images, vertical T1WI and T2WI images, and transverse and vertical enhanced T1WI (Fig. 1). According to these images, clinical doctors could evaluate the location and size of the lesions, and observe their blood supplies and relations with the surrounding tissues.

Characteristics of dynamic contrast-enhanced MRI of the breast diseases. Through dynamic contrast-enhanced MRI of the breast, the blood supply for the lesions, as well as comparison between the lesions and normal tissues was observed to understand different ways of signal enhancement between lesions and normal tissues.

The dynamic enhanced MRI of normal gland tissues showed gradual intensity enhancement. From the first period of contrast agent injection (at about 20th s), minor intensify enhancement was observed and lasted more than 5 to 6 min in some cases. Some cases demonstrated a low level of signal intensity after the initial minor enhancement.

The fat tissues in the contrast enhanced MRI showed no intensity enhancement.

The lesions of breast cancer gradual intensity enhancement from the first period of the contrast agent injection and apparent intensity enhancement in the second period, and reached the peak in the 3rd to 5th period (60th to 100th s) with obvious staining. Then the intensity of the lesions lowered with uneven signals or continued

Table 1 Comparison of MRI and pathological diagnosis in 30 cases with breast lesions

Case number	Age (years)	Tumor number	MRI diagnosis	Pathological diagnosis
1	41	3	Breast cancer with satellite nodules	Infiltrating ductal carcinoma
2	26	1	Fibroadenoma	Fibroadenoma
3	41	1	Benign tumor	Lobule hyperplasia adenositis
4	58	1	Intraductal papilloma	Intraductal papilloma
5	48	1	Malignant tumor	In situ carcinoma with intraductal infiltration
6	40	3	Malignant tumor with two fibromas	One infiltrating ductal carcinoma with two fibromas
7	40	2	Hyperplastic nodules or inflammation	One node of breast fibrocystic hyperplasia and one of lymphadenitis
8	56	1	Benign nodule	Fibrocystic hyperplasia
9	49	1	Breast cancer	Inflammatory breast cancer
10	26	1	Prosthesis	Prosthesis
11	35	1	Breast cyst	Breast cyst
12	46	3	Breast cancer with lymph node metastasis	Two infiltrating ductal carcinomas with one lymph node metastasis
13	33	3	Breast cancer with chest wall invasion and axillary node metastases	Two infiltrating ductal carcinoma with one axillary node and chest wall invasion
14	33	1	Breast cancer	Sclerosing adenositis
15	48	2	Breast cancer with chest wall invasion and axillary node metastases	One infiltrating ductal carcinoma with one axillary node and ectopectoralis invasion
16	36	4	Two fibromas and two intraductal papillomas	Two fibromas and two intraductal papillomas
17	39	1	Breast cancer with dermal papilla invasion	Breast cancer with dermal papilla invasion
18	37	0	Normal	Normal
19	58	0	Normal	Normal
20	46	2	Multiple intraductal papilloma	Two intraductal papillomas
21	35	1	Fibrocystic hyperplasia and fidroma	Fibroadenoma
22	34	2	Diagnosis undermined, maybe malignant	One fibroadenoma and one cyst
23	40	1	Bilateral axillary lymphadenectasis with normal breast	Axillary lymphadenitis
24	67	3	Breast cancer with intraductal dissemination, fibroadenoma	One fibroadenoma, one infitrating ductal carcinoma and one in situ carcinoma
25	33	1	Breast cancer	Infiltrating ductal carcinoma
26	59	2	Breast cancer with intraductal dissemination, fibroadenoma	One fibroadenositis and one infitrating ductal carcinoma
27	37	2	Breast cancer for the right breast nodule, malignancy can not be excluded for the left breast nodule	Two fibroadenomas
28	33	1	Chronic inflammation	Inflammation
29	37	3	Breast cancer and two cysts	One infitrating ductal carcinoma and two cysts
30	55	1	Fibroadenoma	Fibroma

to maintain the state of enhancement (Fig. 2A-C).

Characteristics of post-processing images of MRI of the breast diseases. From the pcolor, the

areas with the most obvious signal changes were observed (Fig. 3).

The subtracted images could vividly reflect the areas of lesions (Fig. 4).

Through the intensity-time curves, the changes of signal intensity at different enhancement phases for lesions or normal tissues were observed to identify increase or decrease of signal intensity in specific time periods (Fig. 5).

The 3D reconstruction images at different planes helped to understand the relation between the lesions and nearby tissues (Fig. 6).

The maximum slope ratio with the distant normal tissues from the lesions as the contrast,

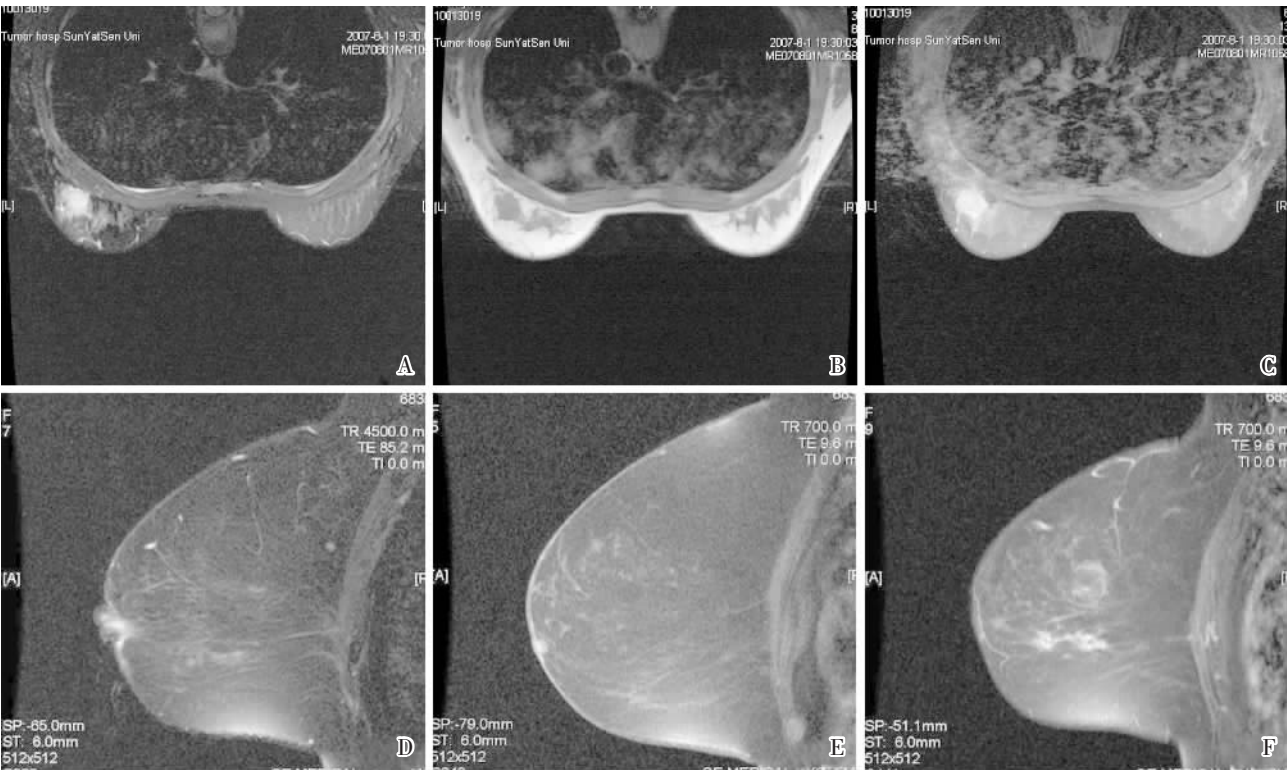


Figure 1 Plain and contrast-enhanced MR images of the breast

A: Axial T2WI image with fat suppression;
 B: Axial T1WI image;
 C: Axial contrast-enhanced T1WI image with fat suppression;
 D: Sagittal T2WI image with fat suppression;
 E: Sagittal T1WI image with fat suppression;
 F: Sagittal contrast-enhanced T1WI image with fat suppression.



Figure 2 Dynamic contrast-enhanced images of the breast

A: Plain scan image;
 B: MR image during the early phase;
 C: MR image during the late phase.

avoided variance of individuals and reflected the characteristics of the lesions in a more accurate manner, thus was more comparable.

To summarize the above diagnosis methods, the diagnosis sensitivity was 100% and the diagnosis accuracy rate was 93.3%.

Discussion

Breast diseases are common, and frequently-occurring diseases in women, which are mostly diagnosed by mammography and

ultrasonography. Since the US Food and Drug Administration (FDA) approved MRI for clinical application in 1984, its relevant techniques and devices have developed rapidly. Especially the development of new imaging techniques and software signals a bright prospect for diagnosis of breast diseases.

The dynamic contrast enhanced breast MRI modality shows potential to predict microvascular density and infiltration velocity of contrast agents in order to objectively reflect the blood supply of breast tumor and to help evaluate biological

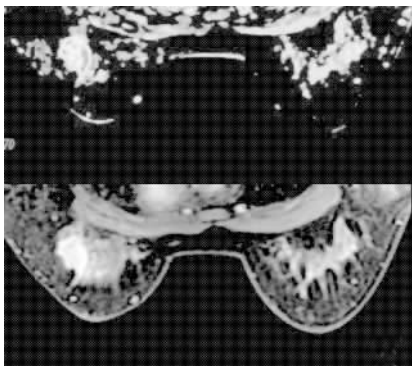


Figure 3 Pseudocolor image of the breast

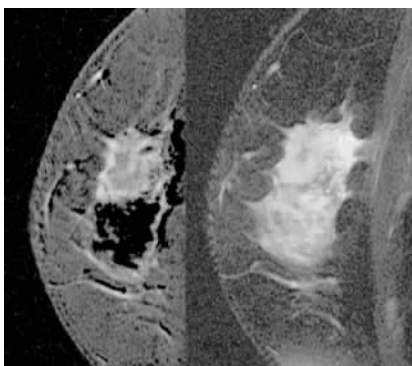


Figure 4 Subtraction image of the breast

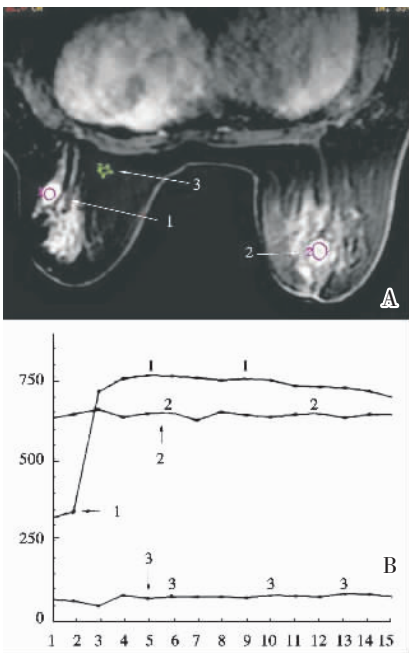


Figure 5 Time-signal intensity curve of the interest area of breast lesions

1. Time-signal intensity curve for the malignant tumor; 2. Time-signal intensity curve for the benign tumor; 3. Time-signal intensity curve for normal tissues. A: MR image for the interest area; B: Time-signal intensity curve.

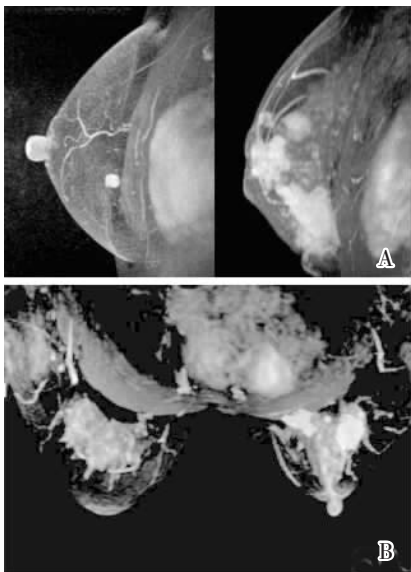


Figure 6 3D reconstruction images of the breast

A: Sagittal image of 3D reconstruction
B: Axial image of 3D reconstruction

behavior plus prognosis of breast tumor.⁷ However, the dynamic contrast enhancement curves alone are influenced by individual variance. Liu et al.⁸ and Guo et al.⁹ found that distribution of the maximum signal intensity and maximum slope between the benign and malignant lesions showed no statistically significant difference, or were even overlapping, indicating that diagnostic accuracy remains to be improved.

Ouyang et al.¹⁰ proposed the maximum slope ratio (Slope^R) besides maximum signal intensity (SI_{max}), enhancement peak (PH) and maximum slope. Slope^R regards normal gland tissues or fat tissues as the contrast for adjustment. It helps to increase diagnosis accuracy rate as it accurately reflects microvascular density and permeability in the lesions as opposed to the normal tissues. The pattern of dynamic contrast enhanced breast MRI can reflect the blood supplies and pharmacokinetic state of the breast lesions, and the post-processing procedures including image subtraction, dynamic curves mapping, and 3D reconstruction help to find and locate and qualitative diagnosis of the lesions. The maximum slope ratio with the distant normal tissues from the lesions as the contrast avoids variance of individuals and reflects the characteristics of the lesions in a more accurate manner, thus was more comparable.

We believe that MRI is a significant diagnosis technique that differentiates benign breast lesions from malignant lesions, guarantees early diagnosis, and evaluates invasion of breast cancer as well as efficacy of treatments for breast cancer. However, due to diversity and complexity of MRI techniques, different researchers with different experience may achieve different information; deviation of results could exist. According to the findings in our study, the subtracted breast MR images can assist in identifying location of lesions. The dynamic curves for lesions can provide information of hemodynamics of the lesions, which promote evaluation of characteristics of lesions. The 3D reconstruction images in the perspective of morphology identify borders of the lesions and vividly demonstrate whether rich blood supply

exists and nearby tissues are invaded. Taking distant normal tissues from the lesions as the contrast compares the blood supplies between the lesions and normal tissues, as well as avoids impact of individual variance.

Plain and dynamic enhanced MRI, as well as post-processing techniques, if applicable, paves a solid foundation for accurate diagnosis of breast diseases.

References

- [1] Li LD, Rao KQ, Zhang SW, et al. Statistical analysis of data from 12 cancer registries in China, 1993–1997[J]. *Zhong Guo Zhong Liu*, 2003, 11(9):497–507. [in Chinese]
- [2] Wang SA, Sun HR, Bai RJ, et al. Clinical application of presaturation pulse for fat Suppression in breast MRI [J]. *Lin Chuang Fang She Xue Za Zhi*, 2004, 23 (1):21–26. [in Chinese]
- [3] Zhao B, Wang GB. The value of MRI on breast lesion[J]. *Yi Xue Ying Xiang Xue Za Zhi*, 2007, 17 (2):109–110. [in Chinese]
- [4] Fischer U, Kopka L, Grabbe E. Breast Carcinoma: effect of preoperative contrast-enhanced MR imaging on the therapeutic approach[J]. *Radiology*, 1999, 213(3):881–888.
- [5] Lou LX, Zhang JJ, Shi GF. Diagnosis of benign and malignant breast lesions by dynamic contrast enhanced MR imaging and digital subtraction imaging [J]. *Lin Chuang Fang She Xue Za Zhi*, 2007, 26(2):148–152. [in Chinese]
- [6] Helbich TH, Becherer A, Trattnig S, et al. Differentiation of benign and malignant breast lesions: MR imaging versus Tc-99m sestamibi scintimammography [J]. *Radiology*, 1997, 202 (2):421–429.
- [7] Kuhl C, Mielcareck P, Klaschnik S, et al. Dynamic breast MR imaging: are signal intensity time course data useful for differential diagnosis of enhancing lesions? [J]. *Radiology*, 1999, 211(1):101–110.
- [8] Liu PF, Bao RX, Niu Y, et al. Initial investigation on correlation between dynamic contrast enhanced MRI and neovascularization[J]. *Zhonghua Fang She Xue Za Zhi*, 2002, 36(11):967–972. [in Chinese]
- [9] Guo Y, Cai ZL, Cai YQ, et al. Prospective application of dynamic contrast enhanced MRI for differentiation of benign and malignant cancers [J]. *Zhonghua Fang She Xue Za Zhi*, 2001, 9 (35):671–675. [in Chinese]
- [10] Ouyang Y, Xie CM, Wu YP, et al. Dynamic contrast enhanced MRI for differentiation of benign and malignant cancers: use of quantitative parameters and maximum slope ratio[J]. *Zhonghua Fang She Xue Za Zhi*, 2008, 42(6): 569–572. [in Chinese]